Supporting Information for

Polymer-Stabilized Sialylated Nanoparticles: Synthesis, Optimization and Differential Binding to Influenza Hemagglutinins

Sarah-Jane Richards[a], Alexander N. Baker[a], Marc Walker[c] and Matthew I. Gibson[a,b]*

a) Department of Chemistry, University of Warwick, Coventry, CV4 7AL, UK,

b) Warwick Medical School, University of Warwick, Coventry, CV4 7AL, UK

c) Department of Physics, University of Warwick, Coventry, CV4 7AL, UK

Corresponding Author Email, m.i.gibson@warwick.ac.uk

Methods

Gold nanoparticle functionalization using Gal-PHEA polymers

100 µL of 10 mg.mL^{-1} of polymer solution was added to 1 mL of OD 1 particles and left for 30 minutes at room temperature on a tube roller. After 30 mins, particles were centrifuged at 7000 rpm the supernatant was removed and resuspended in 1 mL milliQ H_2O. This was repeated a further two times to ensure complete removal of any unattached polymer. Stability was confirmed using a serial dilution of NaCl from 1 M – 0.016 M.

Amination of sialyllactose

Sialyllactose sodium salt (0.1 g) in a stirred 10 mL aqueous saturated ammonium carbonate for 2 to 5 days, ensuring the solution remains saturated. Reaction completion was determined by mass spectrometry. After reaction completion, the solution was freeze dried. Excess ammonium carbonate was removed by addition of warm methanol. After complete evolution of CO_2 the methanol was removed *in vacuuo.* ESI-MS: ($C_{23}H_{40}N_2O_{18}$) M = 632.23 observed $[M-H]^-$ observed 631.2 ($C_{23}H_{39}N_2O_{18}$).

Lectin induced aggregation studies by Dynamic Light Scattering (DLS)

25 µL of lectin was added to 25 µL of the glycoAuNPs in a disposable, ultralow volume plastic cuvette to give the indicated concentrations. Average diameter measurements were taken every 30 seconds for 1 hour at 37 °C.

X-ray Photoelectron Spectroscopy (XPS)

The X-ray photoelectron spectroscopy (XPS) data were collected at the Warwick Photoemission Facility, University of Warwick. The samples were attached to electrically-conductive carbon tape, mounted on to a sample bar and loaded in to a Kratos Axis Ultra DLD spectrometer which possesses a base pressure below 1 x 10^-10 mbar.

XPS measurements were performed in the main analysis chamber, with the sample being illuminated using a monochromated Al Kα x-ray source. The measurements were conducted at room temperature and at a take-off angle of 90° with respect to the surface parallel. The core level spectra were recorded using a pass energy of 20 eV (resolution approx. 0.4 eV), from an analysis area of 300 microns x 700 microns. The spectrometer work function and binding energy scale of the spectrometer were calibrated using the Fermi edge and 3d{5/2} peak recorded from a polycrystalline Ag sample prior to the commencement of the experiments. In

order to prevent surface charging the surface was flooded with a beam of low energy electrons throughout the experiment and this necessitated recalibration of the binding energy scale. To achieve this, the C-C/C-H component of the C 1s spectrum was referenced to 285.0 eV. The data were analysed in the CasaXPS package, using Shirley backgrounds and mixed Gaussian-Lorentzian (Voigt) lineshapes. For compositional analysis, the analyser transmission function has been determined using clean metallic foils to determine the detection efficiency across the full binding energy range.

Additional Figures

Size of particles made by step growth method of Bastús *et al*.[1] as determined by UV-vis (estimated using method of Haiss *et al*.[2]) and DLS.

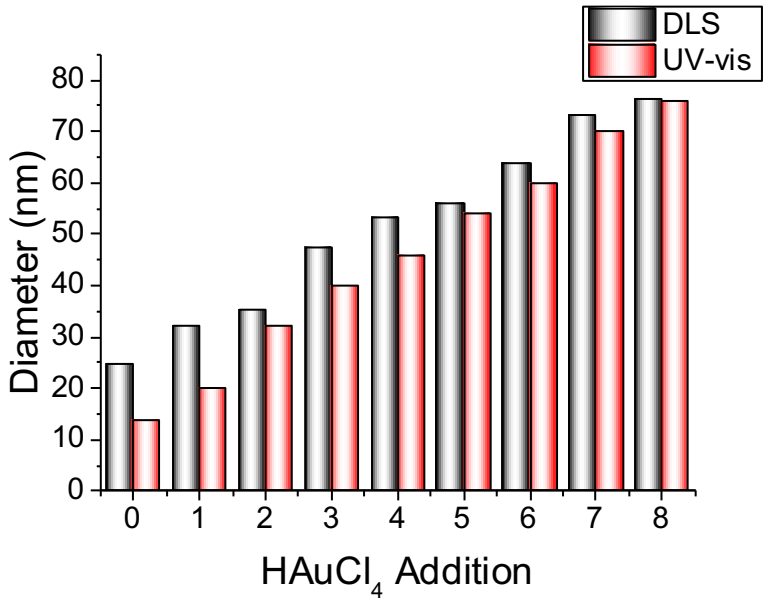

Figure S1. Particle diameters of the gold nanoparticles obtained from the iterative synthetic method. Generations 2, 5 and 7 were used for this study.

X-Ray Photoelectron Spectroscopy (XPS) of Polymer-Coated Particles

Polymer coating was further confirmed by use of XPS. In particular, the presence of amides [from N1s], that are not present on the naked particles, confirmed successful incorporation of the polymers onto the particle surface.

Table S1. Elemental compositions of particles from XPS

	Particle		Particle composition (%)			
AuNP (nm)	**pHEA DP**	**Sugar**	**Au 4f**	**C 1s**	**N 1s**	**O 1s**
30	**No polymer**	**Gal**	16.5	53.95	1.64	27.91
30	**25**	**Gal**	7.07	61.12	4.85	26.96
30	**30**	**Gal**	5.06	62.22	4.36	28.36
30	**35**	**Gal**	6.77	57.39	4.48	31.36
30	**40**	**Gal**	5.09	60.56	4.23	30.12
30	**45**	**Gal**	3.81	68.9	3.78	23.51
50	**No polymer**	**Gal**	9.35	52.58	1.43	36.65
50	**25**	**Gal**	12.38	59.23	6.33	22.06
50	**30**	**Gal**	8.43	56.23	5.86	29.48
50	**35**	**Gal**	9.54	58.05	6.04	26.36
50	**40**	**Gal**	5.19	59.53	5.35	29.94
50	**45**	**Gal**	5.00	60.33	4.26	30.41
70	**No polymer**	**Gal**	5.34	55.82	5.03	33.81
70	**25**	**Gal**	6.792	57.28	4.62	31.31
70	**30**	**Gal**	4.21	56.69	4.38	34.72
70	**35**	**Gal**	7.34	56.51	5.26	30.89
70	**40**	**Gal**	6.60	59.04	3.95	30.41
70	**45**	**Gal**	13.49	56.27	4.45	25.78
70	**25**	**2,3 sialic acid**	5.75	44.25	2.87	47.13
70	**25**	**2,6 sialic acid**	6.10	45.3	3.34	45.27

Table S2. Au:N intensity ratios from XPS

AuNP (nm)	Particle pHEA DP	Sugar	Intensity ratio Au 4f :N 1s
30	**No polymer**	**Gal**	90.99:9.01
30	**25**	**Gal**	59.31:40.69
30	**30**	**Gal**	53.73:46.27
30	**35**	**Gal**	60:19:39.81
30	**40**	**Gal**	54.65:45.35
30	**45**	**Gal**	50.18:49.82
50	**No polymer**	**Gal**	86.76:13.24
50	**25**	**Gal**	66.16:33.84
50	**30**	**Gal**	58.97:41.03
50	**35**	**Gal**	61.23:38.77
50	**40**	**Gal**	49.24:50.76
50	**45**	**Gal**	54.03:45.97
70	**No polymer**	**Gal**	51.51:48.49
70	**25**	**Gal**	59.52:40.48
70	**30**	**Gal**	48.99:51.01
70	**35**	**Gal**	58.29:41.71
70	**40**	**Gal**	62.60:37.40
70	**45**	**Gal**	75.20:24.80
70	**25**	**2,3 sialic acid**	66:67:33.33
70	**25**	**2,6 sialic acid**	64.61:35.39

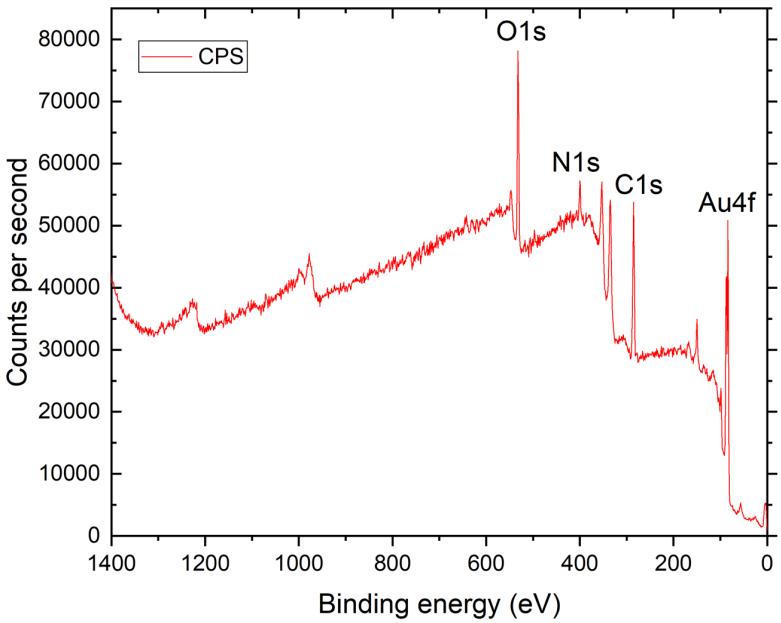

Figure S2. Representative XPS survey scan of Gal-PHEA$_n$@AuNP$_x$ (Gal-PHEA$_{30}$@AuNP$_{50}$)

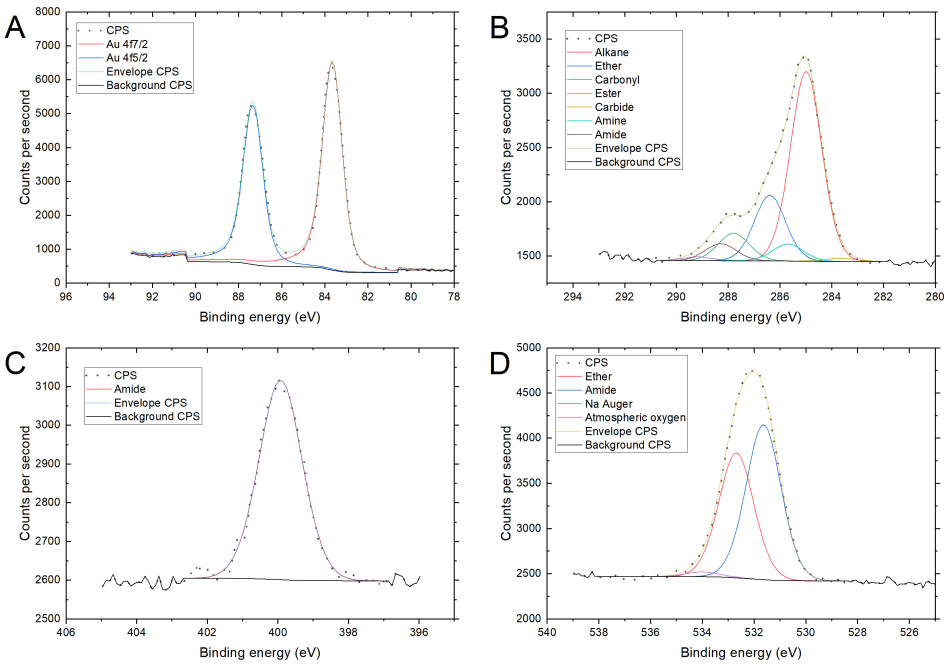

Figure S3. Representative XPS of Gal-PHEA$_n$@AuNP$_x$ (Gal-PHEA$_{30}$@AuNP$_{50}$)

A) Au4f B) C1s C) N1s D) O1s

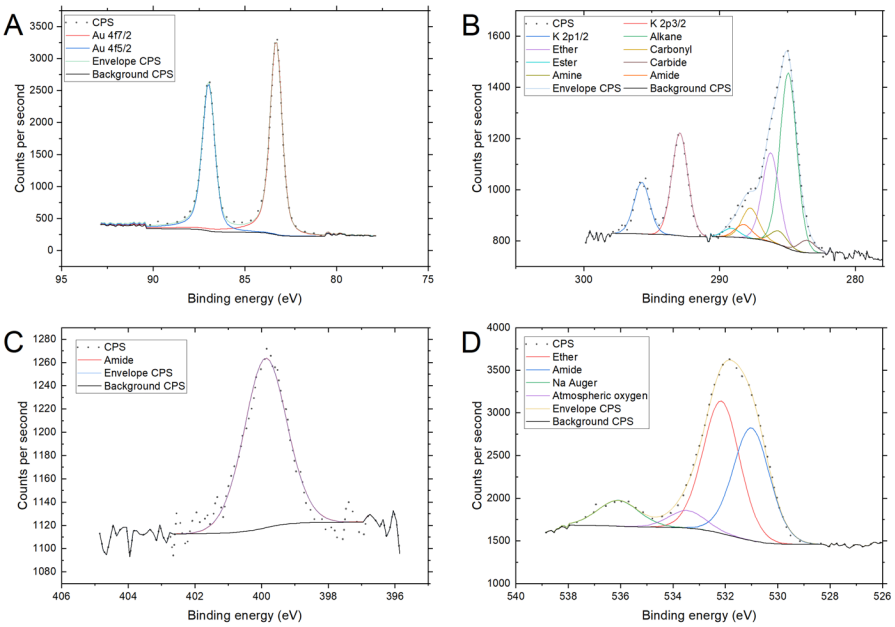

Figure S4. XPS of 2,3-SL-PHEA$_{25}$@AuNP$_{70}$ A) Au4f B) C1s C) N1s D) O1s

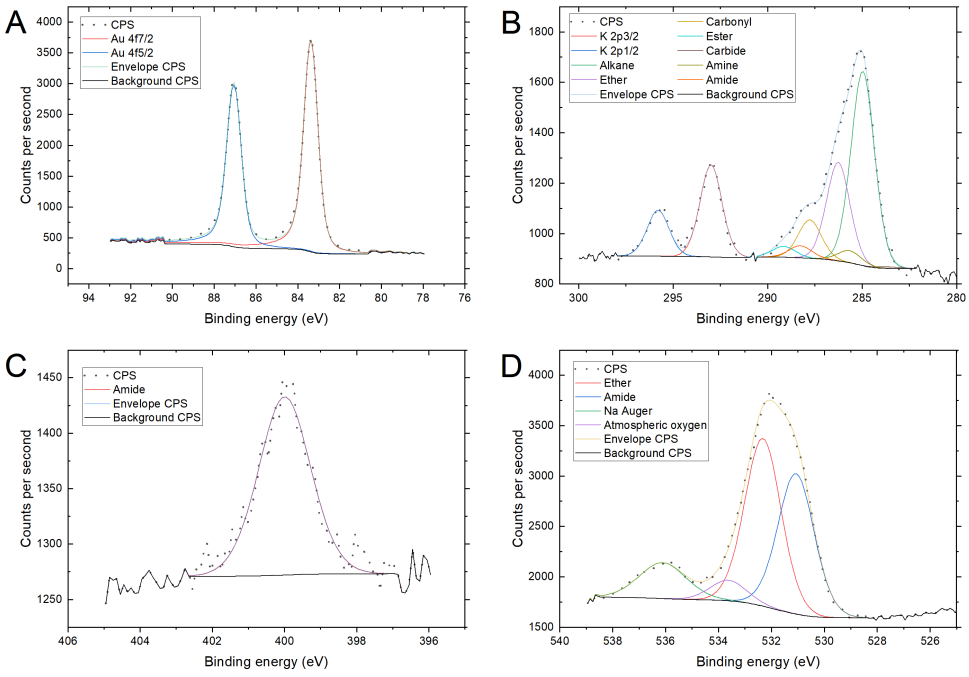

Figure S5. XPS of 2,6-SL-PHEA$_{25}$@AuNP$_{70}$ A) Au4f B) C1s C) N1s D) O1s

Colloidal Stability of Particles

The effect of linker length and particle size on saline stability was determined by exposing the particles to a gradient of saline and monitoring the change in absorbance at 700 nm. No change, indicates a stable colloid.

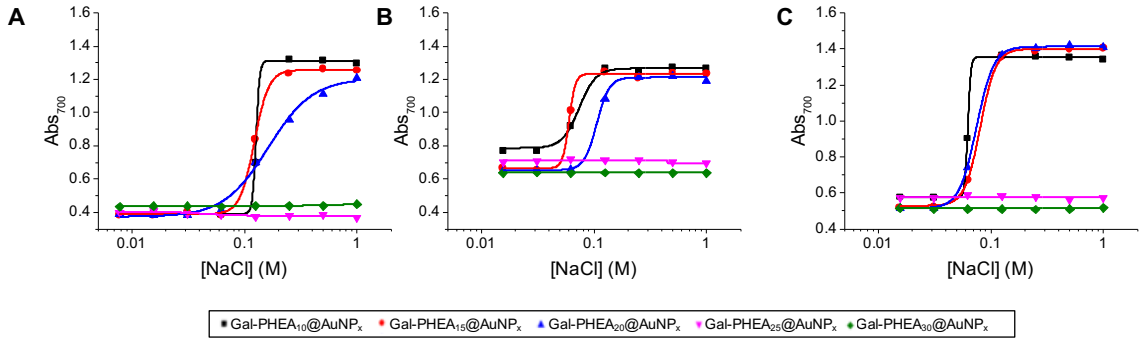

Figure S6. Abs700 as a function of NaCl concentration for different sizes of nanoparticles. A = 30 nm, B = 50 nm, C = 70 nm. Where x = AuNP size

Particles with a linker shorter than DP25 were unstable in saline conditions used for the determination of interaction therefore for all further studies only linkers DP25 and above were used.

Binding isotherms for the aggregation of particles induced by SBA

As part of the screening (summarized in Figure 2B in main text) full binding isotherms for galactosylated nanoparticles against SBA were obtained, shown below.

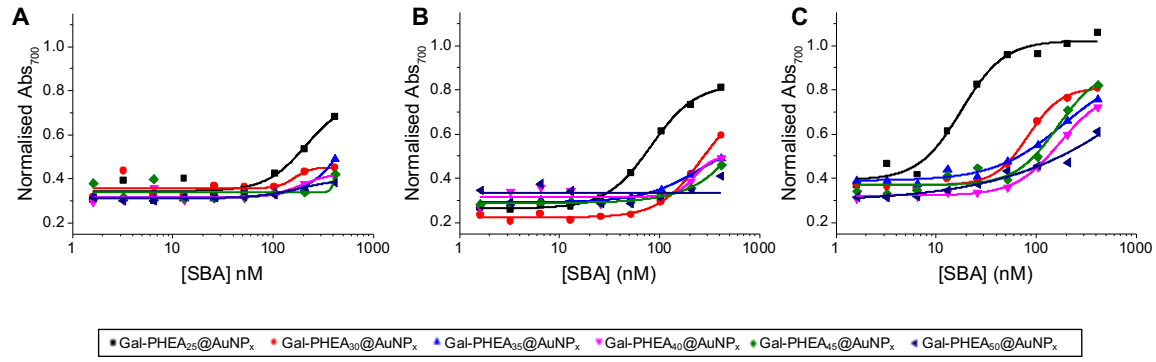

Figure S7. Dose dependent response of SBA to each galactosylated nanoparticle as a function of chain length and size. A = 30 nm; B = 50 nm; C = 70 nm. Where x = AuNP size

Biolayer interferometer

As part of the screening (summarized in Figure 2D in main text) biolayer interferometry association/dissociation curves for galactosylated nanoparticles to SBA coated biosensors were obtained, shown below.

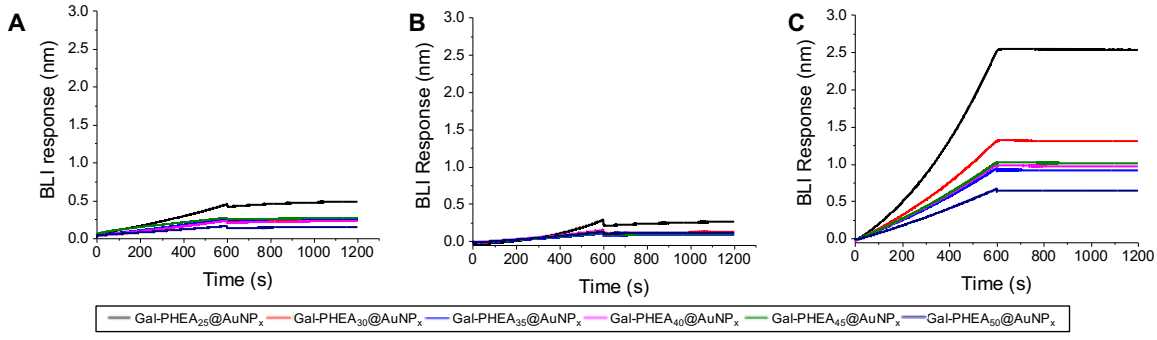

Figure S8. BLI response of SBA-functionalized sensors with different nanoparticles. A = 30 nm; B = 50 nm; C = 70 nm. Where x = AuNP size

DLS

The aggregation of particles upon addition of SBA was confirmed by DLS by measuring size distributions every 1 minute for 15 minutes.

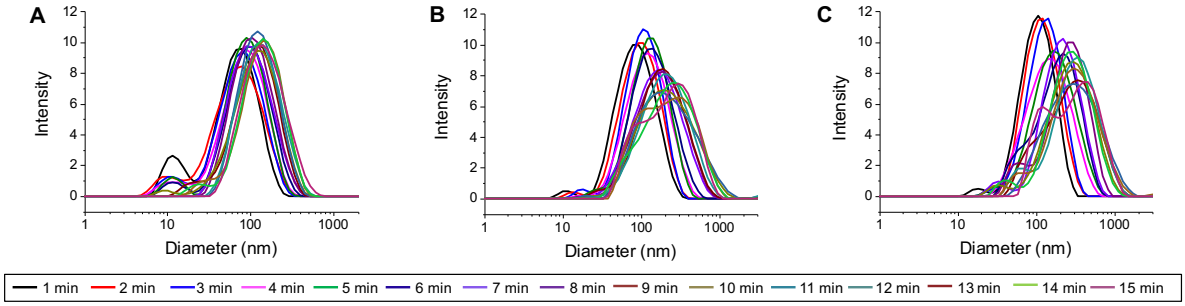

Figure S9. Aggregation of Gal-PHEA$_{25}$@AuNPx with 0.1 mg/mL^{-1} SBA by DLS . A = 30 nm; B = 50 nm; C = 70 nm.

Correlation function graphs of the particles (from S9) aggregating over 15 minutes.

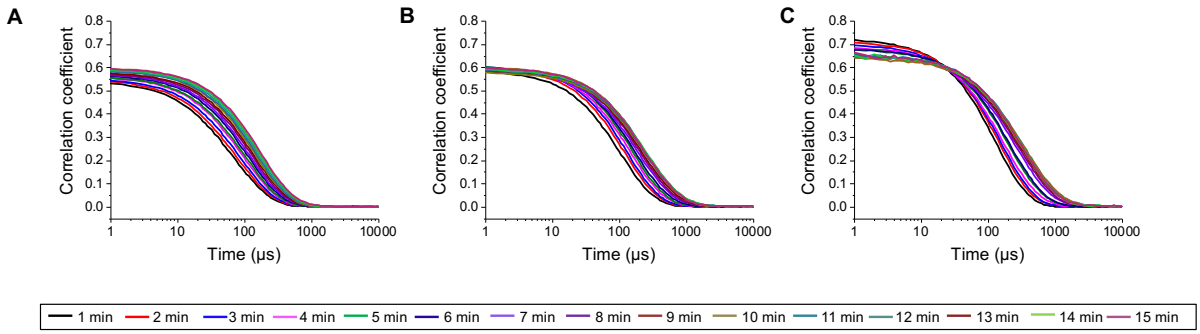

Figure S10. Correlation functions for DLS graphs shown in Figure S6 Aggregation of Gal-PHEA25@AuNPx with 0.1 mg/mL^{-1} SBA. A = 30 nm; B = 50 nm; C = 70 nm.

WGA-induced aggregation of sialylated- and galactosylated- AuNPs

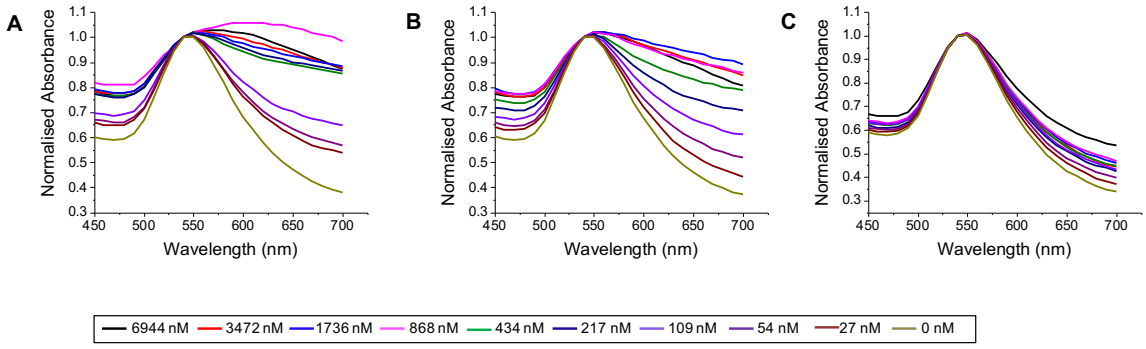

Figure S11. UV-vis spectra of nanoparticles in response to WGA. A) 2,6-SL-PHEA$_{25}$@AuNP$_{70}$ B) 2,3-SL-PHEA$_{25}$@AuNP$_{70}$ C) Gal-PHEA$_{25}$@AuNP$_{70}$.

Influenza Hemagglutinin Screening

Following the hemagglutinin panel screen (in main text), H1, H7 and H9 were interrogated further with a dilution series of 2,6- and 2,3-SL-PHEA$_{25}$@AuNP$_{70}$.

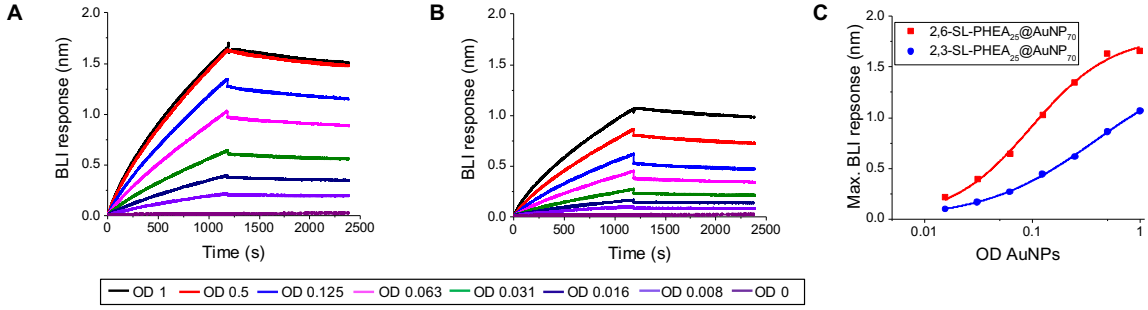

Figure S12. Response of A) 2,6-SL-PHEA$_{25}$@AuNP$_{70}$ and B) 2,3-SL-PHEA$_{25}$@AuNP$_{70}$ to H1 functionalized BLI biosensors. C) Maximum BLI response vs AuNP concentration.

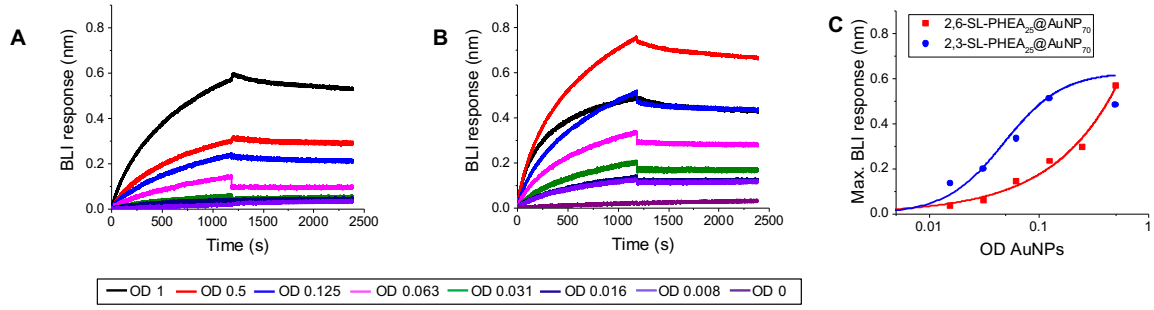

Figure S13. Response of A) 2,6-SL-PHEA$_{25}$@AuNP$_{70}$ and B) 2,3-SL-PHEA$_{25}$@AuNP$_{70}$ to H7 functionalized BLI biosensors. C) Maximum BLI response vs AuNP concentration.

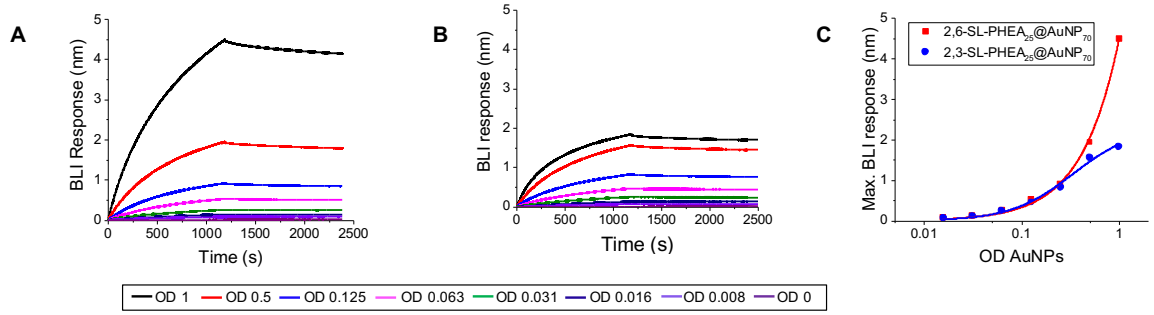

Figure S14. Response of A) 2,6-SL-PHEA$_{25}$@AuNP$_{70}$ and B) 2,3-SL-PHEA$_{25}$@AuNP$_{70}$ to H9 functionalized BLI biosensors. C) Maximum BLI response vs AuNP concentration.

References

(1) Bastús, N. G.; Comenge, J.; Puntes, V. Kinetically Controlled Seeded Growth Synthesis of Citrate-Stabilized Gold Nanoparticles of up to 200 Nm: Size Focusing versus Ostwald Ripening. *Langmuir* **2011**, *27* (17), 11098–11105.

(2) Haiss, Wolfgang; Thanh, N. T. K. .; Aveyard, J. and; Fernig, D. G. Determination of Size and Concentration of Gold Nanoparticles from UV−Vis Spectra. *Anal. Chem.* **2007**, *79* (11), 4215–4221.